International Journal of Innovative Environmental Studies Research 14(4):72-92, Oct-Dec., 2026

© SEAHI PUBLICATIONS, 2026 www.seahipublications.org ISSN: 2354-2918

DOI:10.5281/zenodo.23894981

Subsoil Characterization Using Geophysical and Geotechnical Investigations for Structural investigation in Abdullahi Fodio University of Science and Technology Aliero

U. Z. Magawata; A. A. Gado & A. A. Yahaya

Department of Physics, Abdullahi Fodio University of Science and Technology, Aliero Nigeria.
Correspondence; zayyanu.magawata@ksusta.edu.ng

ABSTRACT

Subsurface heterogeneity can significantly influence foundation performance, particularly in sedimentary terrains where variations in lithology, moisture content, and soil strength may cause differential settlement and structural instability. This study integrates two-dimensional electrical resistivity tomography (ERT) and geotechnical investigations to characterize subsurface conditions beneath selected buildings at Abdullahi Fodio University of Science and Technology, Aliero, northwestern Nigeria. Three approximately 200 m electrical resistivity profiles were acquired using the Wenner electrode configuration and processed through two-dimensional inversion. Compaction and direct shear tests were conducted to determine maximum dry density, optimum moisture content, cohesion, and angle of internal friction. The resistivity models reveal considerable subsurface variability, with values ranging from approximately 17.6 to over 1,000 Ωm, potentially reflecting differences in lithology, clay content, moisture conditions, weathering, and cementation. Maximum dry density ranges from 1.70 to 2.10 g/cm³, optimum moisture content from 9.6 to 16.9 %, cohesion from 2.0 to 36.4 kPa, and angle of internal friction from 6° to 25°. Calculated allowable bearing capacities range from 104.55 to 197.60 kN/m². Administrative Block III records the lowest value, while Science Block I records the highest. The result reveal the complementary value of geophysical and geotechnical methods for preliminary foundation assessment. Further subsurface verification and settlement analysis are recommended to support reliable foundation design.

Keywords: Electrical resistivity tomography; subsurface characterization; geotechnical properties; soil shear strength; bearing capacity; foundation stability; Gwandu Formation.

INTRODUCTION

All geophysical techniques rely on detecting variations in the physical properties of subsurface materials (Kassymkanova et al., 2023; Rahimi et al., 2024; Elshalkany et al., 2025). They are widely applied in environmental, groundwater, and engineering investigations to characterize subsurface geology, groundwater occurrence, aquifer geometry, and groundwater quality (Usman, 2019; Kumar et al., 2024; Olasunkanmi et al., 2023; Mensah et al., 2024; Magawata and Lawal, 2025; Usman et al., 2026). Their non-invasive nature and relatively low cost make them valuable for foundation assessment, particularly given increasing concerns about building failures in Nigeria (Oyedele and Olorode, 2011; Abija, 2023). Conventional site investigation methods include cone penetration testing (CPT), standard penetration testing (SPT), trenching, and laboratory soil analysis (Akintorinwa and Adesoji, 2009; Oyedele, 2013;

Magawata et al., 2020). Integrating these methods with geophysical techniques provides a better understanding of subsurface conditions. Geophysical methods are widely used in groundwater exploration, building-site investigations, and dam and dike inspection (Klimis et al., 1999; Sarvaidis et al., 1999; Luna and Jadi, 2000). They also help identify cavities, fractures, faults, lithological contacts, and heterogeneous foundation materials that may compromise structural stability (Venkateswara, et al., 2004; Othman, 2005; Soupios et al., 2005). Electrical resistivity methods identify subsurface variations associated with lithology, porosity. Also, two-dimensional (2D) resistivity imaging delineates lateral and vertical variations, while vertical electrical sounding (VES) establishes geoelectric sequences (Olabode and Sand 2023; Ojo et al., 2024; Olatunji et al., 2025). Their integration with geotechnical testing improves subsurface characterization, although resistivity alone cannot conclusively determine soil strength or foundation competence. Previous studies have investigated foundation instability using integrated geophysical and geotechnical methods (Akintorinwa and Adelusi, 2009; Ofomola et al., 2009; Egwuonwu, and Osazuwa 2011; Bayode et al., 2012; Sumonu et al., 2013; Oyedele, 2013; Samuel et al., 2018; Muhammad, et al., 2019). Despite previous research in Nigeria and some part of the world, site-specific investigations remain essential for assessing existing structures and guiding future construction. At Abdullahi Fodio University of Science and Technology, Aliero, integrated geophysical and geotechnical investigations are necessary to characterize subsurface materials, identify possible geological structures, and evaluate foundation conditions. Further subsurface investigations have also been recommended in recent studies (Alao and Abubakar, 2025; Ishimwe et al., 2026). Therefore, this study integrates 2D electrical resistivity imaging, and geotechnical laboratory testing to assess subsurface conditions beneath some selected low-rise buildings at Abdullahi Fodio University of Science and Technology, Aliero, Kebbi State, Nigeria. It aims to delineate conductive zones and possible geological structures, establish the geoelectric sequence, evaluate soil engineering properties, and assess their implications for foundation stability. The results may also provide supplementary information on groundwater-related features and support future construction planning.

2.0 Location and Geological Setting of the Area

The study area is located within the northwestern region of Nigeria, specifically in Kebbi State, which lies at the southern margin of the Iullemmeden Basin (also known as the Sokoto Basin). The Sokoto Basin is one of the major sedimentary basins in Nigeria, covering an approximate area of 60,000 square kilometers and extending into the Republic of Niger to the north (Obaje, 2022). The local geology is dominated by the Gwandu Formation, which overlies the older sedimentary units and the basement rocks in an unconformable relationship (Figure 1). The Gwandu Formation in this area consists predominantly of continental deposits including sandstones, siltstones, claystones, and lateritic soils, deposited in fluvial and lacustrine environments during the Tertiary to Quaternary periods (Obaje, 2022).

The Gwandu Formation is characterized by significant lateral and vertical facies variations, with alternating sequences of coarse-grained sandstones (potential aquifer units) and fine-grained claystones and siltstones (aquitard units). The sandstone units are typically friable to moderately consolidated, with variable porosity and permeability depending on the degree of cementation and the presence of clay matrix. The claystone units act as confining layers that can create confined or semi-confined aquifer conditions in the underlying sandstone units (Adeyemi et al., 2021).

Lateritic soils and ferruginous crusts are extensively developed on the surface in the Aliero area, formed through prolonged tropical weathering processes. These lateritic materials can vary in thickness from a few meters to over 20 meters and may exhibit variable hydraulic properties depending on their degree of induration and the presence of relict structures (Obaje, 2022). The lateritic cover can influence groundwater recharge processes, with well-developed lateritic profiles potentially impeding infiltration and promoting surface runoff, while fractured and brecciated laterites may enhance recharge through preferential flow paths.

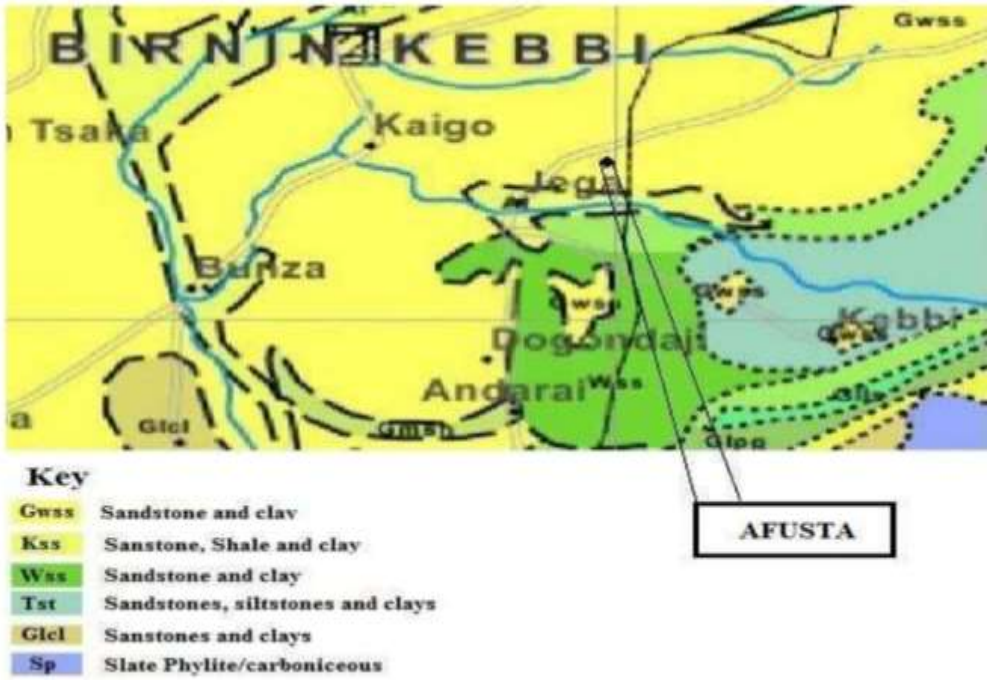

Figure 1: Geological map of the study area after (NGSA 2009).

3.0 MATERIAL AND METHODS

3.1. Two Dimensional Electrical Resistivity Imaging Approach

The direct-current electrical resistivity method was employed using the Wenner electrode configuration to investigate subsurface resistivity variations. Three NW–SE-oriented profiles, each with a spread length of approximately 200 m, were established to cross the major structural trend in the study area. Equidistant electrode spacing (a) of 1, 3, 5, 10, and 15 m were used to investigate lateral and vertical variations in subsurface resistivity. Resistance (R) measurements were converted to apparent resistivity (rho) using the appropriate geometric factor (K), as expressed in Equations (1) and (2). The Wenner configuration provides sensitivity to subsurface resistivity variations associated with changes in lithology, porosity, moisture content, and permeability, as well as possible geological discontinuities, fractures, and faults. During data acquisition, direct current was injected into the ground through the current electrodes, while the resulting potential difference was measured between the potential electrodes. The apparent resistivity was subsequently calculated from the measured resistance and the geometric factor, following the approach described by Loke and Barker (1996). The acquired apparent-resistivity data were processed using Res2DINV software to generate two-dimensional (2D) inverse resistivity models, which were used to interpret the lateral and vertical distribution of subsurface resistivity and infer possible geological variations within the investigated area.

Equations

$$pa = KR \qquad 1$$

For the Wenner configuration:

$$K = 2\pi a \qquad 2$$

Where pa is the apparent resistivity (Ω m), K is the geometric factor (m), R is the measured resistance (Ω), and a is the equal spacing between adjacent electrodes (m).

3.2 Geotechnical approach

3.2.1 Soil Sampling

This involve digging of one meter trial pits at strategic location inside Abdullahi Fodio University of science and technology, Aliero Nigeria. Soil samplings will be carried out progressively during the trial pit digging. Ordinary disturbed samples was taken at the anomalous ERT location be taken at change of strata as deemed necessary and bulk samples will be collected within the trial pit. The sampling locations and their coordinates are as follows; Multipurpose hall (Latitude: N 12˚ 18' 17.0" Longitude: E 4˚ 29' 48.76"), Physical Sciences; (Latitude: N 12˚ 18' 24.373" Longitude: E 4˚ 29' 44.81") Administrative block (Latitude: N 12˚ 18' 23.453" Longitude: E 4˚ 29' 35.84").

3.2.2 Sample preparation

The Nigerian standard for soil test methods was followed in preparing the remoulded soil specimens using a controlled moisture content method. The soil was remoulded, and its dry density was adjusted to approximate the in-situ dry density. Specimen preparation involved the following four steps:

(i) Soil drying: The soil sample was dried in an electric blast drying oven.

(ii) Sieving: The dried soil sample was crushed and passed through a 2 mm sieve.

(iii) Moisture conditioning: Distilled water was uniformly added to the sieved soil to achieve the required moisture content. The prepared soil was then placed in a sealed plastic bag and left for 72 h to ensure uniform moisture distribution.

(iv) Specimen compaction: Based on the specimen dimensions and target moisture content, the required mass of soil was calculated and compacted in five equal-mass layers. Each layer was compacted to achieve the specified density, and its surface was scarified before placing the next l.ayer to ensure proper bonding between adjacent layers. After compaction of the final layer, the specimen ends were trimmed and levelled, and the specimen was weighed to ensure that the mass remained within the allowable tolerance. The main specimen preparation procedure is illustrated in Fig 2.

3.2.3 Direct Shear Test Procedure

The direct shear test was conducted to determine the shear-strength parameters of the soil, namely cohesion (c) and the angle of internal friction (φ). Representative soil specimens were prepared to fit a shear box consisting of two halves capable of moving horizontally relative to each other. The specimen dimensions and initial conditions were recorded, including whether the sample was disturbed or

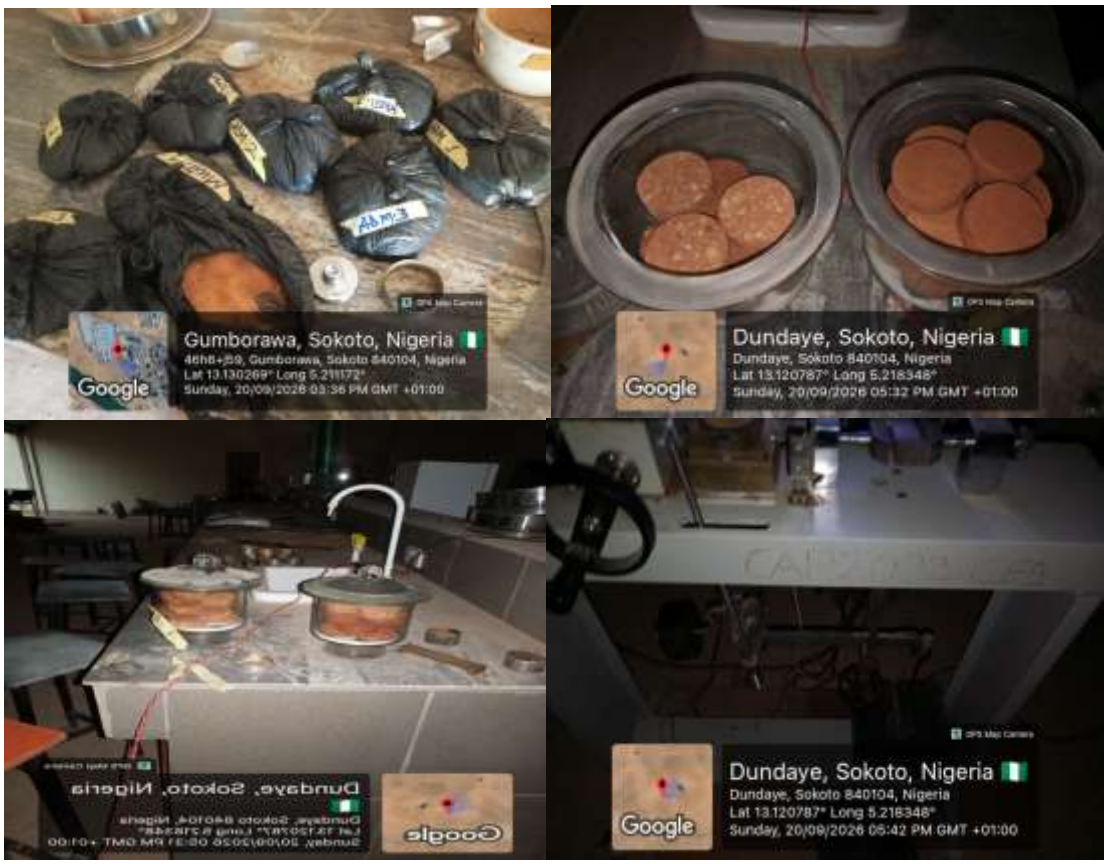

Fig 2: Illustration of the main specimen preparation procedure.

undisturbed and whether it was tested in a dry, moist, or saturated condition. The specimen was placed in the shear box, and a predetermined normal load was applied. The corresponding normal stress was calculated by dividing the applied normal force by the relevant specimen area. Where applicable, the specimen was allowed to consolidate under the applied normal load in accordance with the adopted test procedure.

Shearing was performed by moving one half of the shear box horizontally at a prescribed displacement rate while maintaining the normal load. The shear force and horizontal displacement were recorded throughout the test. The peak shear force, or the failure value defined by the adopted criterion, was identified and used to calculate the corresponding shear stress, with the necessary correction for changes in specimen area. The test was repeated on comparable specimens under different normal stress levels to

obtain the corresponding failure shear stresses and establish the soil failure envelope. The actual number of specimens, applied normal stresses, displacement rate, drainage conditions, and test standard should be reported based on the laboratory records, as these details cannot be determined from the cohesion and friction-angle values alone. The direct shear test also, provides preliminary information about resistance to shearing under applied normal stress. The principal parameters are cohesion (c) and angle of internal friction (φ), represented by the Mohr–Coulomb equation:

$$\tau f = c + \sigma n \tan \varphi \qquad 3$$

Here, τf is shear strength at failure and σn is normal stress. Greater cohesion and friction angle can contribute to greater shear resistance, but the combined effect depends on normal stress, drainage, soil condition, and whether the reported failure envelope is valid.

3.2.3.1 Determination of Cohesion and Friction Angle

Normal stress and shear stress at failure are calculated as follows:

$$\sigma n = \frac{Fn}{A} \qquad 4$$

$$\tau f = \frac{Fs}{A} \qquad 5$$

$$\tau f = c + \sigma n \tan \varphi \qquad 6$$

$$\varphi = \tan^{-1}(\text{slope}) \qquad 7$$

Here, Fn is the applied normal force, Fs is the shear force at failure, and A is the relevant shear-plane area (with any area correction required by the test method). Plot failure shear stress (τf) on the vertical axis against normal stress (σn) on the horizontal axis and fit a straight line. The vertical-axis intercept gives cohesion (c), while the angle of internal friction (φ) is the inverse tangent of the fitted line's slope. Use effective-stress symbols only if the reported parameters are effective-stress parameters; otherwise, define them as total-stress values.

3.2.3.2 Bearing-Capacity Method

The supplied calculations use Terzaghi's bearing-capacity equation for a shallow strip footing. Confirm that this footing model is appropriate before presenting it as the adopted method.

$$Qult = cNc + qNq + 0.5\,\gamma\,B\,N\gamma \qquad 8$$

$$q = \gamma\,Df \qquad 9$$

$$Qult = cNc + \gamma\,Df\,Nq + 0.5\,\gamma\,B\,N\gamma \qquad 10$$

Where qult is ultimate bearing capacity (kN/m²), c is cohesion (kN/m²), Nc, Nq and Nγ are bearing-capacity factors, q is surcharge pressure at foundation level (kN/m²), γ is soil unit weight (kN/m³), B is footing width (m), and Df is foundation depth (m). Obtain the factors from the same Terzaghi formulation or factor table, using the measured friction angle.

RESULT AND DISCUSSION

4.1 The 2D electrical Resistivity Tomography (ERT)

The inverted Wenner resistivity sections reveal substantial lateral and vertical variations in subsurface resistivity across the investigated portions of the Gwandu Formation, Sokoto Basin north western Nigeria. These variations indicate differences in subsurface material composition and potentially in the engineering properties of the underlying sediments. The Gwandu Formation comprises sandstone inter bedded with clay stone, mudstone and other fine-grained sediments; consequently, variations in clay content, moisture conditions, grain size and cementation may account for the observed resistivity contrasts. These characteristics are important in engineering site investigations because weak or compressible clay-rich materials and heterogeneous weathered sediments may contribute to differential settlement, whereas dense, well-cemented sandstone or lateritic materials may provide comparatively competent foundation support, subject to confirmation by geotechnical testing.

4.1.1 Profile 1

The inverse model indicates a relatively low-resistivity zone of approximately 17.6–203 Ωm, extending broadly between 35 and 125 m along the profile and occurring through much of the investigated depth, locally approaching 30 m (Figure 3). This zone may represent clay-rich sandstone, silty clay or mudstone, although moisture content and groundwater conditions may also influence the measured response. From an engineering perspective, if these materials are confirmed to be clay-rich and compressible, they may exhibit relatively low bearing resistance or greater settlement potential under structural loading. However, low resistivity alone cannot establish the strength or compressibility of the material. In contrast, the western part of the profile, approximately 0–40 m, contains a pronounced high-resistivity anomaly, with values locally exceeding 1,000 Ωm. Additional high-resistivity anomalies occur between approximately 125 and 185 m. These zones may represent relatively clean sandstone, ferruginized sediments or strongly cemented materials that could provide more competent foundation conditions if they are sufficiently dense and mechanically sound. Nevertheless, high resistivity may also reflect dry or fractured materials and should not be regarded as direct evidence of high bearing capacity.

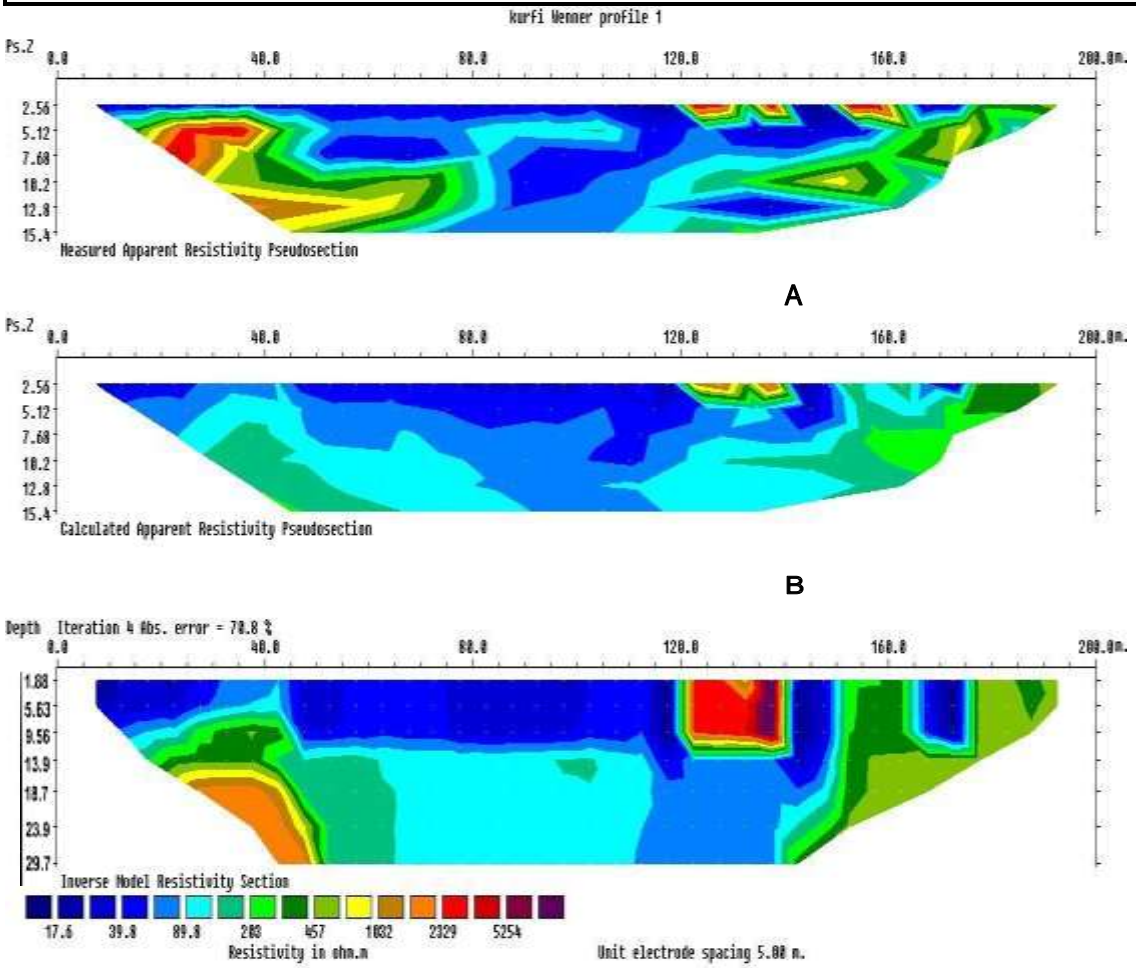

Figure 3 (a) calculated (b) Measured (c) Inverse model of profile 1

4.1.2 Profile 2

Profile 2 exhibits a broad resistive zone at the western end, approximately 0–40 m, where resistivity locally exceeds several hundred Ωm and reaches values above 1,000 Ωm. A relatively resistive to intermediate-resistivity body extends through approximately 30–100 m, with portions of the anomaly occurring within the upper 10–13 m of the model (Figure 4). These materials may correspond to sandstone-rich or ferruginized sedimentary units and could provide favourable foundation conditions where confirmed to be dense and competent. However, the central portion, approximately 100–145 m, is characterized by relatively low resistivity, represented by the blue-to-cyan colors on the inverted section. This zone may indicate clay-rich sediments or other conductive materials. If geotechnical investigation confirms the presence of soft or compressible clay, the zone may be associated with increased settlement potential and reduced suitability for conventional shallow foundations without appropriate design measures. Toward the eastern end, approximately 150–200 m, a relatively high-resistivity body occurs adjacent to a pronounced resistivity transition. This contrast may indicate a change in lithology or degree of cementation, suggesting potentially variable foundation conditions across relatively short distances. Such lateral heterogeneity is relevant to building design because differential settlement may develop where foundations rest on materials with contrasting stiffness or compressibility.

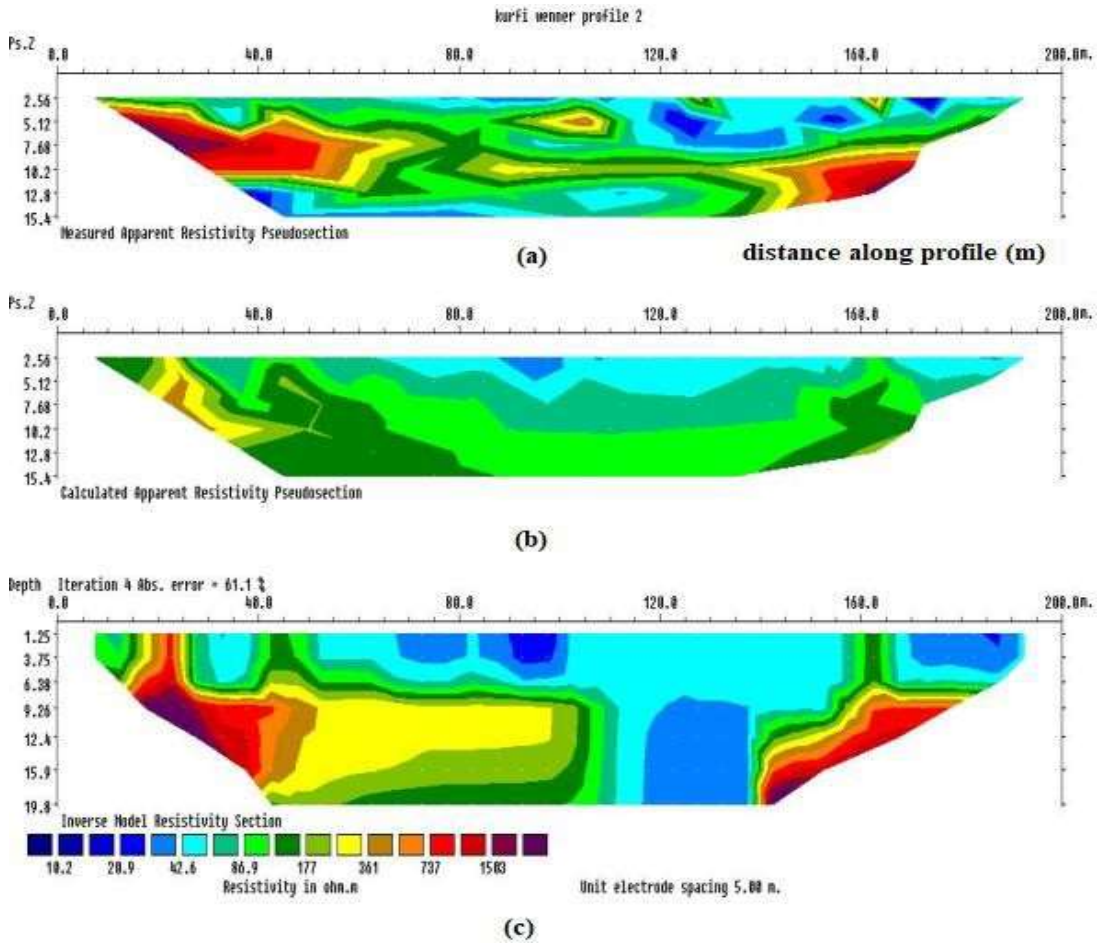

Figure 4: (a) calculated (b) Measured (c) Inverse Model of Profile 2

4.1.3 Profile 3

The electrical resistivity imaging profile extends for approximately 200 m and images the subsurface to a nominal depth of about 19 m (Figure 5). The measured apparent-resistivity pseudosection (a) displays marked lateral and vertical variation, indicating that the subsurface is electrically heterogeneous rather than composed of a single uniform layer. The calculated apparent-resistivity pseudosection (b) represents the response predicted from the inversion model. Its broad spatial correspondence with the measured section suggests that the model reproduces the principal pattern of the field data, although local differences remain. The inverse-model resistivity section (c) provides the principal basis for geological interpretation.

The inverse model shows a relatively low-to-moderate resistivity zone across much of the shallow section, interrupted by localized higher-resistivity bodies and underlain by a broad, more resistive domain that becomes especially prominent from approximately 100–180 m along the profile. The color scale spans roughly 4 to several thousand Ω m (as labelled on the supplied figure). The lowest-resistivity colors occur mainly in shallow and localized zones, whereas the highest-resistivity colors form a substantial deeper body in the central-to-eastern part of the section. These boundaries should be treated as gradational geophysical transitions, not as exact geological contacts.

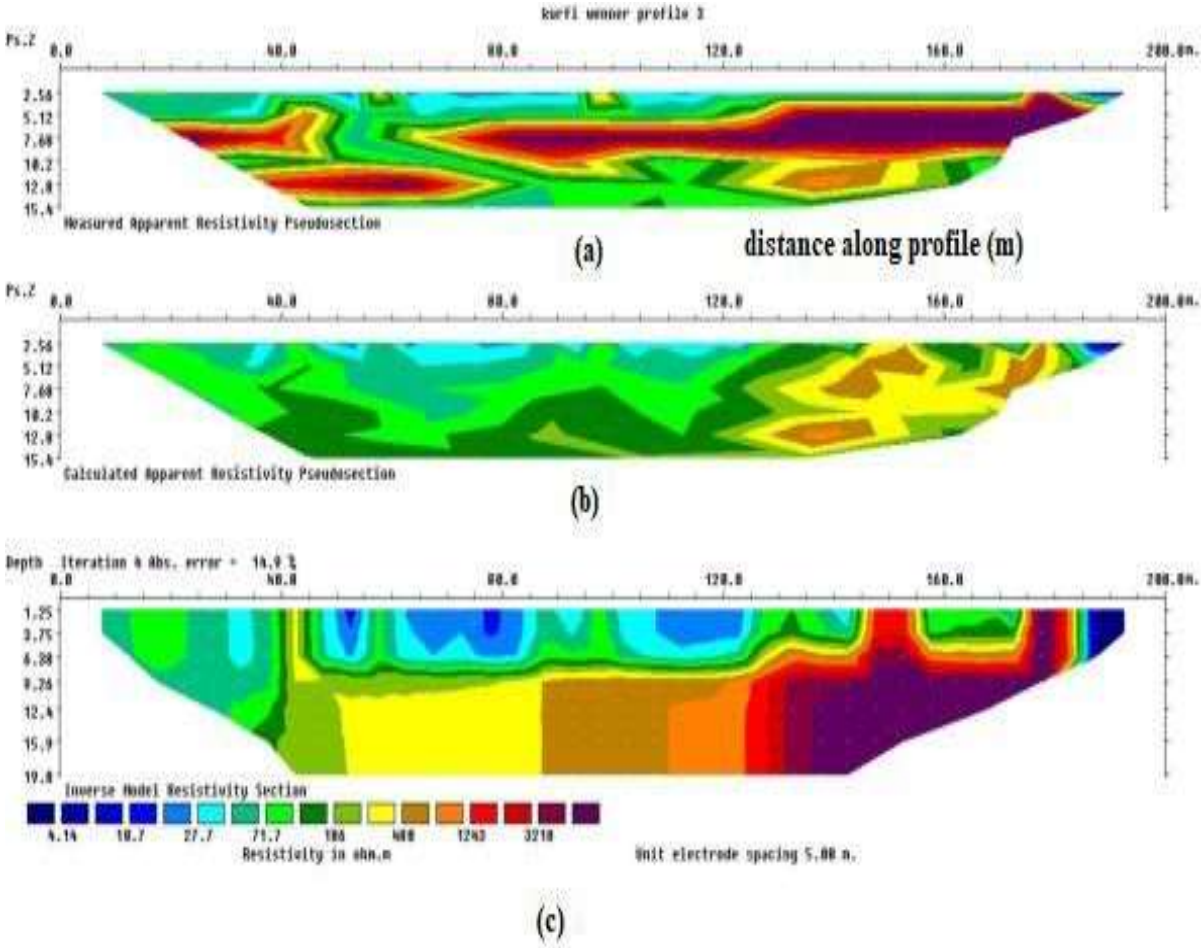

Figure 5: *(a) calculated (b) Measured (c) Inverse Model of Profile 3*

4.2 Geotechnical Soil Analysis

4.2.1 Compaction

Compaction results describe the dry density attainable under a specified laboratory effort, whereas bearing capacity depends on shear strength, foundation geometry, embedment depth, groundwater conditions, and loading. A high maximum dry density (MDD) alone does not establish high allowable bearing capacity (Table 1).

Table 1: The MDD and optimum moisture content (OMC) values below are transcribed from the reported laboratory results.

Location/sample	MDD (g/cm³)	OMC (%)	Preliminary interpretation
Multi-Purpose I	1.74	9.6	relatively low MDD; low moisture demand
Multi-Purpose II	1.92	10.6	relatively high MDD; low-to-moderate OMC
Multi-Purpose III	1.82	16.9	Moderate MDD; comparatively high OMC
Admin Block I	1.94	14.1	High MDD; moderate-to-high OMC
Admin Block II	1.81	11.5	Moderate MDD and OMC
Admin Block III	1.70	14.0	Lowest reported MDD
Science I	2.10	13.2	Highest reported MDD
Science II	1.82	12.0	Moderate MDD and OMC
Science III	1.98	11.8	High MDD; relatively low OMC

4.2.2 Multi-Purpose Building

Multi-Purpose II recorded an MDD of 1.92 g/cm³, higher than Multi-Purpose I (1.74 g/cm³) and Multi-Purpose III (1.82 g/cm³). This suggests that Sample II achieved a denser packing arrangement under the reported laboratory conditions. Its OMC of 10.6 % is lower than the 16.9 % reported for Sample III. The lower MDD of Multi-Purpose I may reflect differences in grading, plasticity, particle composition, or compaction response; it does not independently prove that the soil is weak or unsuitable.

4.2.3 Administrative Block

Admin Block I recorded an MDD of 1.94 g/cm³, followed by Admin Block II at 1.81 g/cm³ and Admin Block III at 1.70 g/cm³. Admin Block I therefore had the highest reported dry-density potential within this location, while Admin Block III had the lowest. Moisture conditioning and field compaction control warrant attention at Admin Block III. Soil classification and field density measurements are needed before judging suitability.

4.2.4 Science Block

Science I recorded the highest reported MDD (2.10 g/cm³), followed by Science III (1.98 g/cm³), while Science II recorded 1.82 g/cm³. These results suggest greater laboratory dry-density potential for Science I and Science III than for Science II. Science I may be a candidate for engineered fill or compacted subgrade if field density testing confirms the result. A high MDD does not guarantee high foundation bearing capacity. Across the nine samples, reported MDD ranges from 1.70 to 2.10 g/cm³ and OMC ranges from 9.6 % to 16.9 %. Science I has the highest reported MDD (2.10 g/cm³), while Admin Block III has the lowest (1.70 g/cm³). These variations indicate different compaction responses. Values should be verified where original readings or curves appear inconsistent.

4.3 Shear test

The direct shear test results reveal appreciable spatial variability in the shear strength characteristics of the soils sampled from the Multipurpose, Administrative, and Science Block locations. The measured cohesion values range from 2.0 to 36.4 kN/m², while the reported angles of internal friction range from 6° to 25°. The unit weights vary between 20.8 and 24.0 kN/m³, indicating differences in the physical and mechanical characteristics of the sampled soils.

The Multipurpose Block samples exhibit cohesion values of 2.6–7.2 kN/m² and friction angles of 22–25°. Multipurpose II records the highest friction angle (25°) within this group, together with a cohesion of 2.6 kN/m² and a unit weight of 23.5 kN/m³. These results indicate that frictional resistance may make a substantial contribution to the shear strength of these samples. Under increasing normal stress, their measured shear stresses generally increase, reflecting the expected response of soil under direct shear loading.

The Administrative Block samples exhibit relatively low friction angles of 20–21°, with cohesion values ranging from 2.2 to 10.0 kN/m². Administrative II has the highest cohesion in this group (10.0 kN/m²), whereas Administrative III has the lowest (2.2 kN/m²). This contrast suggests that the soils do not possess uniform shear strength characteristics across the sampled locations. Such variability is relevant to foundation design because the mechanical response of shallow foundations depends on the strength properties of the soil supporting each foundation element.

The Science Block samples display the widest contrast in cohesion, ranging from 2.0 to 36.4 kN/m², and friction angles from 6° to 22°. Science II records the highest cohesion (36.4 kN/m²) but the lowest friction angle (6°), whereas Science III exhibits a cohesion of 2.0 kN/m² and a friction angle of 22°. This contrasting behavior is particularly important because the high reported cohesion of Science II does not necessarily imply superior foundation performance under all loading conditions (Table 2). The relative contributions of cohesion and friction must be evaluated together, particularly where the friction angle is unusually low. The reported value for Science II should therefore be verified against the original laboratory records before the result is interpreted conclusively. Generally, the observed variability indicates that assigning a single representative shear strength value to the entire study area could conceal important differences between foundation locations. The findings support location-specific geotechnical characterization rather than assuming uniform subsurface conditions across the campus.

Table 2: Multi-Purpose Building

Sample	Cohesion, c (kPa)	Friction angle, φ (°)
Multi-Purpose I	7.2	22
Multi-Purpose II	2.6	25
Multi-Purpose III	6.0	24

Multi-Purpose II has the highest reported friction angle (25°), suggesting a relatively greater frictional contribution under comparable normal stress, but it has the lowest reported cohesion (2.6 kPa). Multi-Purpose I has a lower friction angle (22°) but higher cohesion (7.2 kPa). Multi-Purpose III has intermediate reported values (Table 3). Multi-Purpose II should not automatically be considered to have the highest bearing capacity on friction angle alone.

Table 3: Administrative Block

Sample	Cohesion, c (kPa)	Friction angle, φ (°)
Admin Block I	6.0	20
Admin Block II	10.0	20
Admin Block III	2.2	21

Admin Block II has the highest reported cohesion (10.0 kPa), while Admin Block III has the lowest (2.2 kPa). Reported friction angles are similar (20–21°). If valid and comparable, cohesion may contribute to differences in estimated shear strength (Table 4). Admin Block I has the highest MDD of the three samples, whereas Admin Block III has the lowest. These observations do not independently establish allowable bearing pressure.

Table 4: Science Block

Sample	Cohesion, c (kPa)	Friction angle, φ (°)
Science I	16.2	20
Science II	36.4	6
Science III	2.0	22

Science I has reported cohesion of 16.2 kPa and friction angle of 20°, while Science III has lower cohesion (2.0 kPa) and a higher friction angle (22°). Science II is an outlier, with reported cohesion of 36.4 kPa and friction angle of 6°. Its listed shear-stress observations also show a non-monotonic pattern across applied normal stresses. The values require verification against original laboratory readings and the method used to obtain c and φ. Science II should not be described as having the highest bearing capacity until the discrepancy is resolved.

4.4 Implications of shear strength variability for bearing capacity

The calculated bearing capacities provide an integrated assessment of how the measured cohesion, friction angle, and unit weight influence the estimated load-bearing resistance of the soils. The analyses were performed for a foundation depth of 1.0 m and a footing width of 1.0 m, using a factor of safety of 2.5. Under these assumptions, the ultimate bearing capacities range from 261.34 to 494.00 kN/m², while the corresponding allowable bearing capacities range from 104.55 to 197.60 kN/m². Consequently, a soil with a relatively high cohesion value may produce a high calculated bearing capacity even when its friction angle is comparatively low. This relationship helps explain the elevated calculated capacity of Science I and the contrasting result for Science II. However, the calculated values should not be interpreted as direct measurements of foundation performance. They represent estimates derived from the adopted bearing capacity equation and input parameters. Their engineering significance therefore depends on the reliability of the laboratory results, the suitability of the selected equation, and the assumptions concerning foundation geometry and subsurface conditions.

4.5 Comparative assessment of the three sampling locations

The calculated allowable bearing capacities demonstrate differences among the three campus locations. The Multipurpose Block samples yield values of 163.52–185.15 kN/m², the Administrative Block samples yield 104.55–150.04 kN/m², and the Science Block samples yield 121.36–197.60 kN/m².

The Multipurpose Block exhibits comparatively consistent allowable bearing capacity values, with a relatively narrow range of 21.63 kN/m². This consistency suggests less variation in the calculated bearing resistance among the three samples than at the other locations, although three samples alone are insufficient to establish the uniformity of the entire subsurface.

The Administrative Block has the lowest overall allowable bearing capacity, with Administrative III recording the minimum value of 104.55 kN/m². Its relatively low cohesion of 2.2 kN/m² and friction angle of 21° contribute to this result under the adopted calculation method. Administrative II, by comparison, yields 150.04 kN/m², reflecting its higher cohesion of 10.0 kN/m². The difference between these samples highlights the importance of accounting for local variations when selecting foundation design parameters.

The Science Block presents the greatest contrast, with allowable bearing capacities ranging from 121.36 to 197.60 kN/m². Science I records the highest value, whereas Science II produces a substantially lower value despite its high reported cohesion. The difference is largely associated with the low friction angle assigned to Science II in the calculation. This reinforces the need to verify the reported friction angle and cohesion before adopting the calculated capacities for engineering design. These comparisons indicate that the relative suitability of the sampled locations cannot be established solely from their average strength parameters. Instead, foundation assessment should consider the variability within each location, the loads imposed by the proposed structures, and the potential for differential settlement.

4.6 Implications for engineering site investigation

For preliminary foundation assessment, the interpreted low-resistivity zones warrant attention because clay-rich, moist or weathered materials can be relatively compressible and may exhibit reduced strength or variable settlement behavior. Conversely, high resistivity should not automatically be equated with high bearing capacity: dry soil, laterite, cemented sandstone and competent rock can all be resistive, but their engineering performance differs. The profile can help identify lateral variability and guide targeted intrusive investigation, but it cannot by itself provide allowable bearing pressure, shear strength, compressibility or settlement estimates. The spatial range in QSAFE suggests that foundation support conditions may vary across the investigated locations. A higher calculated bearing capacity indicates greater resistance to bearing failure under the assumptions used in the calculation, but it does not by itself establish that a site is suitable for a proposed structure. Total and differential settlement, soil compressibility, groundwater conditions, footing dimensions, loading, excavation conditions and the depth of weaker strata must also be assessed. The reported values apply to the stated 1.0 m foundation depth and 1.0 m footing width; they should not be transferred unchanged to other geometries or depths.

5 CONCLUSION

The integrated geophysical and geotechnical investigations conducted at Abdullahi Fodio University of Science and Technology (AFUSTA), Aliero, within the Gwandu Formation of the Sokoto Basin, northwestern Nigeria, reveal spatial variations in subsurface resistivity and calculated soil bearing capacity that may influence foundation performance. The electrical resistivity profiles identify contrasting conductive and resistive zones, potentially reflecting variations in clay content, moisture conditions, weathering and sandstone cementation. The geotechnical results from the nine sampling locations indicate calculated safe bearing capacities ranging from 104.55 to 197.60 kN/m², with the lowest value recorded at Admn. 3 and the highest at Science 1, for a foundation depth and footing width of 1.0 m and a factor of safety of 2.5. These results establish the importance of evaluating foundation conditions at individual locations rather than adopting a uniform bearing-capacity value for the entire study area. Therefore, the outcomes should be considered preliminary, and further correlation with boreholes test and settlement

analysis is recommended. The study demonstrates the complementary value of electrical resistivity and geotechnical methods for preliminary engineering site characterization.

ACKNOWLEDGEMENT.

The authors wish to acknowledge the support of the Tertiary Education Trust Fund (TETFund) through the Institutional-Based Research (IBR) Grant for 2025/2026. They also appreciate the Departments of Civil Engineering at Abdullahi Fodio University of Science and Technology, Aliero (AFUSTA), and Usmanu Danfodiyo University, Sokoto (UDUS), for their assistance with the soil analyses. The authors further acknowledge the Kebbi State Ministry of Solid Minerals for providing the electrical resistivity equipment (terrameter) used for geophysical data acquisition.

REFERENCES

Abija, F. A. (2023). Ground variation, geotechnical uncertainties and reliability of foundation design for sustainable building infrastructures with case histories. *J Mater Sci Eng Technol. https://doi. org/10*, *61440*.

Adelusi, A. O., Adiat, K. A. N., and Amigun, J. O. (2009). Integration of surface electrical prospecting methods for fracture detection in Precambrian basement rocks of Iwaraja area Southwestern Nigeria. Ocean Journal of Applied Sciences 2(3), 265-280.

Akintorinwa O. J. Adelusi, F. A. (2009). Integration of geophysical and geotechnical investigation for a proposed lecture room complex at the Federal University of Technology, Akure, SW, Nigeria. Journal of Applied Sciences, 2(3), PP. 241 –251.

Akintorinwa O. J., Adesoji J. I. (2009). Application of geophysical and geotechnical investigations

Faculty of Science Buildings, Bowen University Temporary Site, Advances in Physics Theories and Applications Iwo. ISSN 2224-719X (Paper) (Online) Vol.25, (Paris, France), .1-2.995 (2018) 012090 doi: 10.1088/1742-6596/995/1/012090.

Alao, J. O., & Abubakar, F. (2025). Groundwater exploration, management strategies and sustainability: Geophysical approaches. *Geosystems and Geoenvironment*, *4*(3), 100395.

Around municipal waste disposal site in Malete southwestern Nigeria. *Arabian Journal of Geosciences*, *16*(4), 273.

Bayode S., Omosuyi G. O., and Abdullahi H. I. (2012). Post-Foundation Engineering Geophysical Investigation in Part of the Federal University of Technology, Akure, South

Clark, L. (1996). Field Guide to Water Wells and Boreholes. John Wiley and Sons: New York. 155p. DOI: 10.28978/nesciences.522158.

Dorbing M. B., and Savit, C. H. (1988). Introduction to geophysical prospecting. 4TH Edition.MC Grow Hill Book Company page 752, 755.

Egwuonwu G.N. and Osazuwa I.B. (2011). Geophysical and Geotechnical Investigation of the Origin of Structural Instabilities Shown on Some Low Rise Buildings in Zaria, North-Western Nigeria**.** The Pacific Journal of Science and Technology –534– Volume 12.Number 2. November 2011. http://www.akamaiuniversity.us/PJST.htm.

Elshalkany, M., Ahmed, M., Sauck, W., Abouelmagd, A., Mansour, S., El-Nekhiely, I. N., & Omar, A. (2025). Geophysical and remote-sensing constraints on the fault controls on groundwater accumulation in basement rock aquifers in Sinai, Egypt. *Surveys inGeophysics*, *46*(3), 627-664.

Fernandes, I., & Chaminé, H. I. (2022). In situ geotechnical investigations. Advances on testing and experimentation in civil engineering: geotechnics, transportation, hydraulics and natural resources, 29-54.

Fraser D. C., (1989). Contouring of VLF-EM Data, Geophysics. Vol.54.No.2. P.245-253.

Ishimwe, H., Francese, R., De Araujo, O. S., & Valentino, R. (2026). Geophysical Methods for Geotechnical Parameters′ Estimation in Shallow Subsurface Investigations: AReview. *International Journal of Geophysics*, *2026*(1), 7178040.

Kassymkanova, K. K., Istekova, S., Rysbekov, K., Amralinova, B., Kyrgizbayeva, G., Soltabayeva, S., & Dossetova, G. (2023). Improving a geophysical method to determine the boundaries of ore-bearing rocks considering certain tectonic disturbances. *Mining of Mineral Deposits*, *17*(1), 17-27.

Kassymkanova, K. K., Istekova, S., Rysbekov, K., Amralinova, B., Kyrgizbayeva, G., Soltabayeva, S., & Dossetova, G. (2023). Improving a geophysical method to determine the boundaries of ore-bearing rocks considering certain tectonic disturbances. *Mining of Mineral Deposits*, *17*(1), 17-27.

Klimis, N. S., Papazachos, C. B., and Effremidis, C. F. (1999). Determination of the Behavior of a Sedimentary Rock Mass: Comparison of Measured Static and the Dynamic Properties. Proceeding of 9 International Conference on Rock Mechanics

Kumar, S., Manga, M., Nair, A. M., Dixit, A., & Mahanta, C. (2024). Water geochemistry and stable isotope changes record groundwater mixing after a regional earthquake in Northeast India. *Geochemistry, Geophysics, Geosystems*, *25*(7), e2024GC011476.

Loke, M. H., & Barker, R. D. (1996). Rapid least-squares inversion of apparent resistivitypseudosections by a quasi-Newton method1. *Geophysical prospecting*, *44*(1), 131-152.

Luna R., and Jadi, H. (2000). Determination of Dynamic Soil Properties Using Geophysical Methods. Proc. 1 Int. Conference on the Application of Geophysical and NDT Methodologies to Transportation Facilities and Infrastructure Geophysics (Federal highway Administration, Saint Louis, MO), 3, 1-15.

Magawata U. Z, Gulma M. Y, Bawallah M. A, and Ilugbo S. O. (2020). Geotechnical investigationof Sub-Base and Sub-Material of Kali collapse dam Aliero north western Nigeria, usingLaboratory investigation, science journal of Advanced and cognitive research, 2020, 1(1): 61-75 ISSN, 54-54

Magawata, U. Z., & Lawal, M. M. (2025). Geophysical and physicochemical investigation for Groundwater ssessment: A case study of Abdullahi Fodio University of Science and Technology, Aliero Nigeria. 225-241.SEAHI PUBLICATIONS, 2025www.seahipublications.org ISSN: 2354-291.

Mensah, V., Boateng, C. D., Gidigasu, S. S., Wemegah, D. D., Aryee, J. N., Osei, M. A., & Afful,S. K. (2024). Groundwater Exploration Methods in West Africa: A Review.

Mohammed, M. A., Saad, R., Ismail, N. A., Muhammad, S. B., Taib, A., & Saidin, M. (2019).Subsurface soil evaluation using seismic refraction tomography and standard penetration test at Bukit Bunuh Impact Crater Area. *Natural and Engineering Sciences*, *4*(1), 1-10.

Nigeria Geological Survey Agency (NGSA) (2009). Geological Map of Nigeria (2009 Ed.).Published by the Authority of the Federal Republic of Nigeria. p. 1.

Ojo, O. T., Chiaka, I. J., & Mark, A. I. (2024). Geophysical subsurface mapping using the electrical resistivity technique: A comprehensive study of the Petroleum Training Institute maincampus in Effurun. *Indonesian Journal of Earth Sciences*, *4*(1), A846-A846.

Olasunkanmi, N. K., Usman, Z. M., & Jimoh, A. A. (2023). Investigation of groundwater quality around municipal waste disposal site in Malete southwestern Nigeria. *Arabian Journal of Geosciences*, *16*(4), 273.

Olatunji, S., Olasunkanmi, N. K., Magawata, U. Z., & Adeleke, A. E. (2025). Subsurface characterization for foundation valuation of existing engineering structures in basement complex of southwestern Nigeria. *Geofísica internacional*, *64*(2), 1533-1542.

Omolaiye, G. E., Oniyangi, A. K., ISSA, T. A., & Adam, S. B. (2024). Subsurface investigation for pre-foundation study utilizing integrated geophysical and geotechnical methods, UNILORIN campus. *Discover Geoscience*, *2*(1), 101.

Othman, A. A. (2005). Constructed Geotechnical Characteristics of Foundation Beds by Seismic Measurements. Journal of Geophysics, England, l.2, 126-38.

Oyedele K. F. (2013). Identification of competent geologic layers using geophysical and geo-Engineering methods at okunmopo, Lagos Nigeria. International Journal of Advanced Scientific and Technical Research Issue 3, volume 4, July-August 2013.

Oyedele K. F., and Olorode D. O. (2011). Site investigations of subsurface conditions using electrical Resistivity method and cone penetration test at Medina Estate, Gbagada, Lagos, Nigeria. World App Science Journal 11: 1097-1104.

Rahimi, M., Wood, C. M., & Kallivokas, L. F. (2024). A comparative study of using geophysical methods for imaging subsurface voids of various sizes and at different depths. *Engineering Geology*, *341*, 107711. Resistivity Geophysical Methods, J. Balkan Geophysics Society, 2, 128-39.

Rodriguez, M. M. C., & Ferolin, T. P. (2024). Groundwater resource exploration and mapping methods: a review. *Journal of Environmental Engineering and Science*, *19*(3), 140-156.

Samuel, Y. M., Saad, R., Muztaza, N. M., Saidin, M. M., & Muhammad, S. B. (2018, April).Integration of Magnetic and Geotechnical methods for Shallow Subsurface Soil Characterization at Sungai Batu, Kedah, Malaysia. In *Journal of Physics: Conference Series* (Vol. 995, No. 1, p. 012090). IOP Publishing.

Sarvvaidis, A., Tsokas, G., Soupios, P., Vargemezis, G., Manakou, M., Tsourlos, P. and Fikos, Soupios, P., Papazachos, C. B., Vargemezis, G., and Fikos, I. (2005). Application of Modern Seismic Methods for geotechnical Site Characterization. Proc. Int. Workshop in Geo-environment and Geo-technics (Milos Island, Greece, 12-14 September), 163-70.

Soupios, P. M., Papazachos, C. B., Vargemezis, G., & Fikos, I. (2005). Application of seismic methods for geotechnical site characterization. In *International workshop in geoenvironment and geotechnics* (pp. 163-70).

Sumonu L. A, Alagbe, O. A., Mabunmi, S. A., Adeniji, A. A., and Olasunkanmi, N.K. (2013).

University of Technology, Akure Nigeria. The Pacific Journal of Science and Technology. Vol. 10, No. 2, PP. 93 – 110.

Usman L., Magawata., U. Z., Bonde., D. S., Ismail U., Augie., B. G., Sifyanu M., Isah S., andLukman L. K. (2026). Assessment of Solid Waste on Groundwater Quality Using 2D Electrical Resistivity Tomography (ERT) And Water Sample Analysis in Selected Locations of Aliero, Northwestern Nigeria. Research Journal of Pure Science and Technology E-ISSN 2579-0536 P-ISSN 2695-2696, Vol 9. No. 6 2026 www.iiardjournals.org online version. DOI: 10.56201/rjpst.vol.9.no6.2026.pg240.24.

Usman Z. U. (2019). Geoelectric survey for groundwater exploration at Birnin-kebbi, kebbi state, Nigeria. *FUDMA journal of Science*. (FJS) ISSN online: 2616-1370 ISSN print: 2645 – 2944Vol.3 No. 1, (March, 2019), pp 168 -178

Venkateswara, V. R., Srinivasa, R., Prakasa, R. B., and Koteswara, R. P. (2004). Bedrock Investigation by Seismic Refraction Method: A Case Study .J. Ind. Geophysics Union .8, 223-228. Western Nigeria. Journal of Emerging Trends in Engineering and Applied Sciences (JETEAS) 3 (1): 203-210 ©Scholarlink Research Institute Journals, 2012 (ISSN: 2141-7016)

Appendix

DIRECT SHEAR BOX TEST RESULTS

SAMPLE IDENTITY: ***MULTI PURPOSE I***

Test Obs. No.	Displacement (mm) @	Normal Load (Kg)	Normal Stress (kN/m^2)	Shear Load (kN/m^2)	Shear Stress (kN/m^2)	Unit Weight (k/m^3)	Angle of Friction (^{o})	Cohesion (C) (kN/m^2)
1	**4.75**	10	27.25	56	19.16	**22.4**	**22^O**	**7.2**
2		20	54.50	96	32.85			
3		30	81.75	132	45.17			

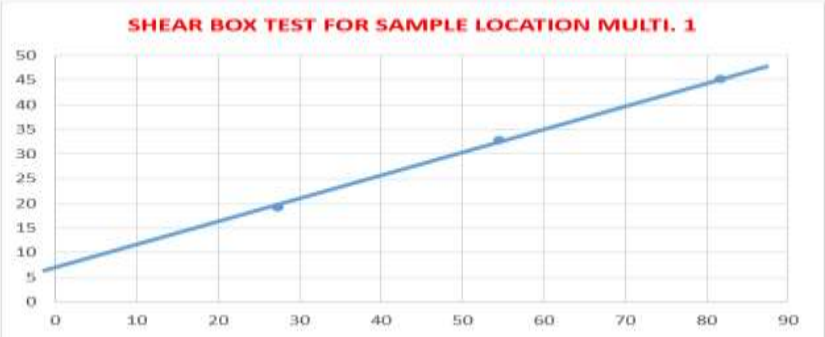

SAMPLE IDENTITY: ***MULTI PURPOSE II***

Test Obs. No.	Displacement (mm) @	Normal Load (Kg)	Normal Stress (kN/m^2)	Shear Load (kN/m^2)	Shear Stress (kN/m^2)	Unit Weight (k/m^3)	Angle of Friction (^{o})	Cohesion (C) (kN/m^2)
1	**4.75**	10	27.25	54	18.48	**23.5**	**25^O**	**2.6**
2		20	54.50	89	30.46			
3		30	81.75	162	55.44			

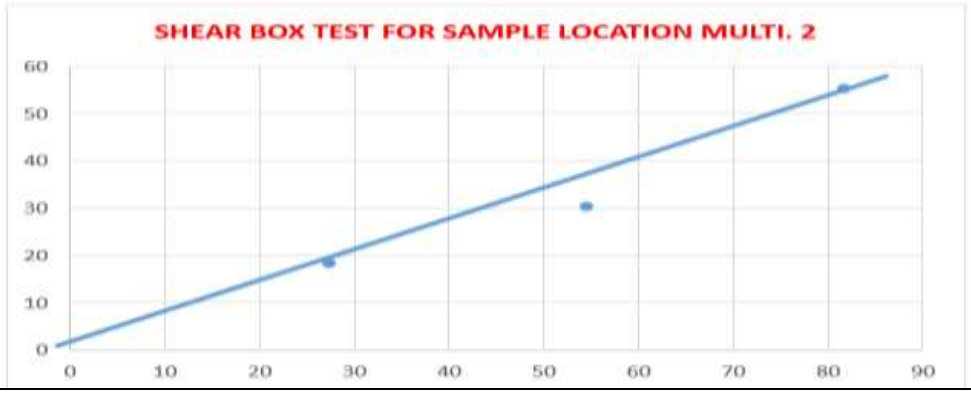

SAMPLE IDENTITY: ***MULTI PURPOSE III***

Test Obs. No.	Displacement (mm) @	Normal Load (Kg)	Normal Stress (kN/m^2)	Shear Load (kN/m^2)	Shear Stress (kN/m^2)	Unit Weight (k/m^3)	Angle of Friction (^{o})	Cohesion (C) (kN/m^2)
1	**4.75**	10	27.25	50	17.11	**21.6**	**24 ^{o}**	**6.0**
2		20	54.50	94	32.17			
3		30	81.75	125	42.78			

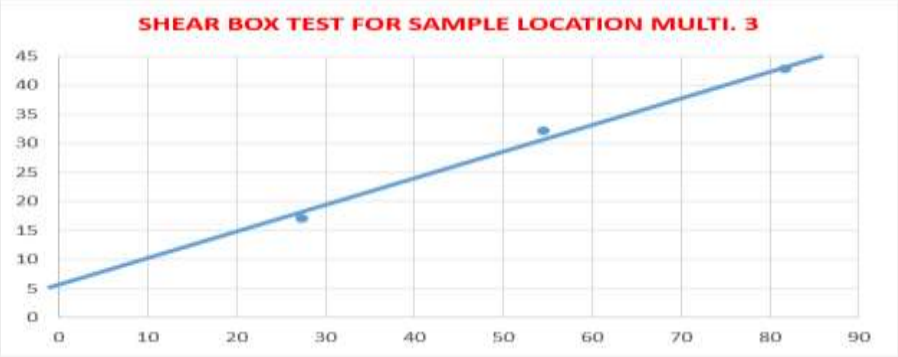

SAMPLE IDENTITY: ***ADMIN BLOCK I***

Test Obs. No.	Displacement (mm) @	Normal Load (Kg)	Normal Stress (kN/m^2)	Shear Load (kN/m^2)	Shear Stress (kN/m^2)	Unit Weight (k/m^3)	Angle of Friction (^{o})	Cohesion (C) (kN/m^2)
1	**4.75**	10	27.25	56	19.16	**20.8**	**20 ^{o}**	**6.0**
2		20	54.50	95	32.51			
3		30	81.75	142	48.59			

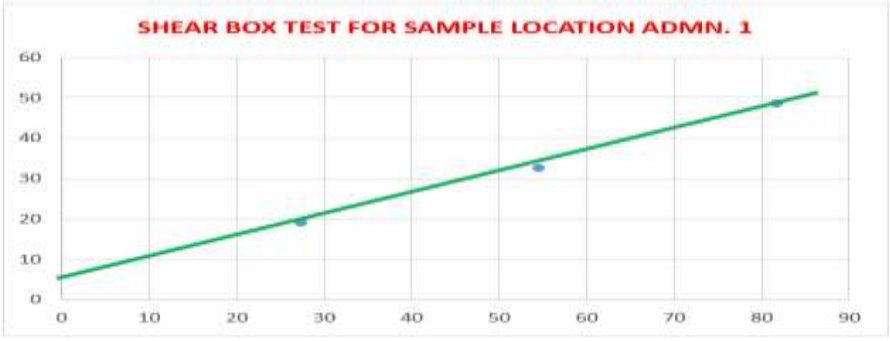

DESCRIPTIONS OF SOIL SAMPLE:
SAMPLE IDENTITY: ***ADMIN BLOCK II***

Test Obs. No.	Displacement (mm) @	Normal Load (Kg)	Normal Stress (kN/m^2)	Shear Load (kN/m^2)	Shear Stress (kN/m^2)	Unit Weight (k/m^3)	Angle of Friction (°)	Cohesion (C) (kN/m^2)
1	**4.75**	10	27.25	64	21.90	**21.4**	**20 °**	**10.0**
2		20	54.50	98	33.54			
3		30	81.75	142	48.59			

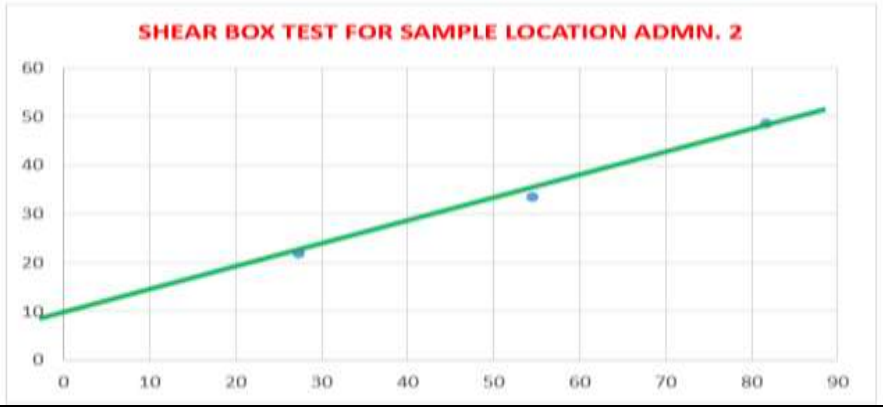

DESCRIPTIONS OF SOIL SAMPLE:
SAMPLE IDENTITY: ***ADMIN BLOCK III***

Test Obs. No.	Displacement (mm) @	Normal Load (Kg)	Normal Stress (kN/m^2)	Shear Load (kN/m^2)	Shear Stress (kN/m^2)	Unit Weight (k/m^3)	Angle of Friction (°)	Cohesion (C) (kN/m^2)
1	**4.75**	10	27.25	49	16.77	**21.1**	**21°**	**2.2**
2		20	54.50	98	33.54			
3		30	81.75	141	48.25			

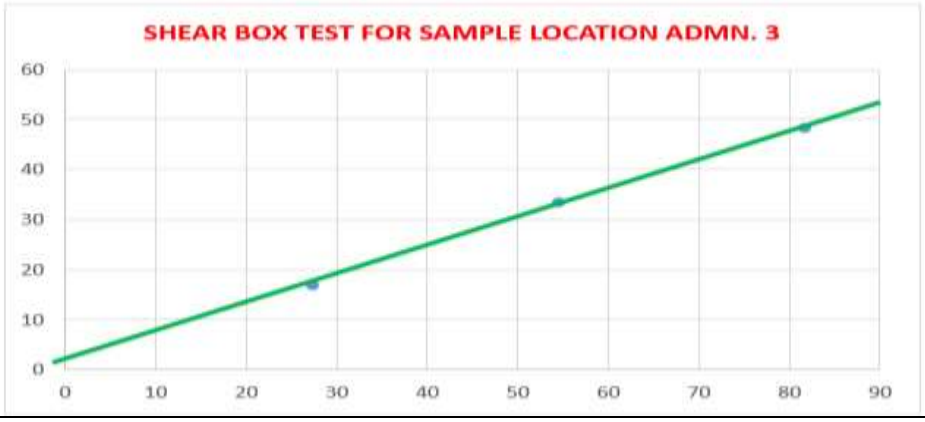

SAMPLE IDENTITY: *SCIENC I*

Test Obs. No.	Displacement (mm) @	Normal Load (Kg)	Normal Stress (kN/m^2)	Shear Load (kN/m^2)	Shear Stress (kN/m^2)	Unit Weight (k/m^3)	Angle of Friction (°)	Cohesion (C) (kN/m^2)
1	**4.75**	10	27.25	94	32.17	**22.4**	**20.0**	**16.2**
2		20	54.50	109	37.30			
3		30	81.75	110	37.65			

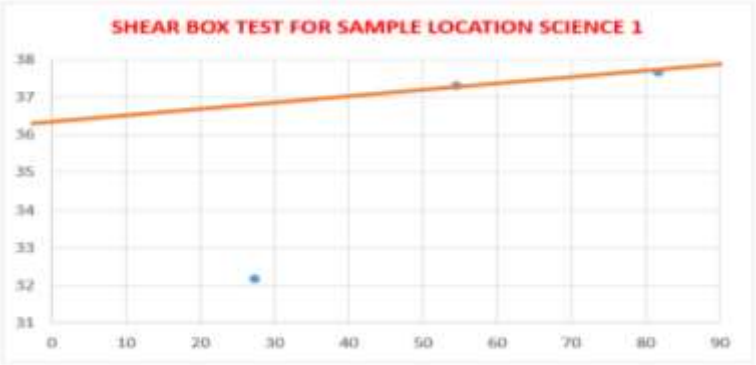

SAMPLE IDENTITY: *SCIENC II*

Test Obs. No.	Displacement (mm) @	Normal Load (Kg)	Normal Stress (kN/m^2)	Shear Load (kN/m^2)	Shear Stress (kN/m^2)	Unit Weight (k/m^3)	Angle of Friction (°)	Cohesion (C) (kN/m^2)
1	**4.75**	10	27.25	113	38.67	**24.0**	**6^o**	**36.4**
2		20	54.50	106	36.28			
3		30	81.75	112	38.33			

SAMPLE IDENTITY: ***SCIENC III***
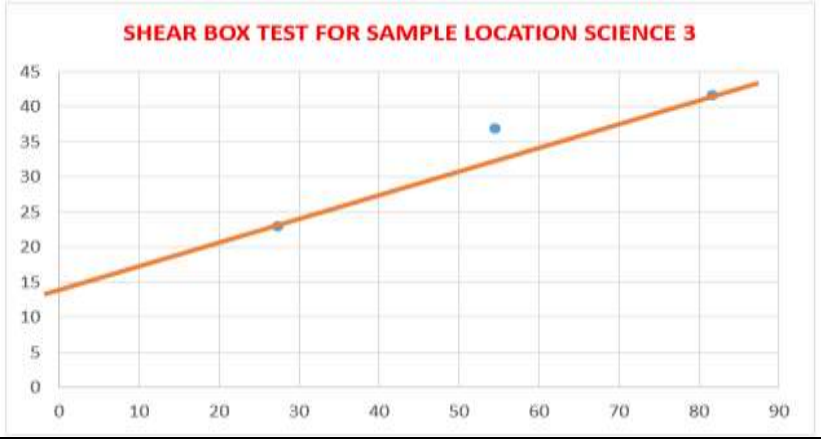
Test Obs. No.	Displacement (mm) @	Normal Load (Kg)	Normal Stress (kN/m^2)	Shear Load (kN/m^2)	Shear Stress (kN/m^2)	Unit Weight (k/m^3)	Angle of Friction (°)	Cohesion (C) (kN/m^2)
1	**4.75**	10	27.25	67	22.98	**22.4**	**22°**	**2.0**
2		20	54.50	108	36.96			
3		30	81.75	120	41.67